Bioorganic & Medicinal Chemistry 28 (2020) 115744

Contents lists available at ScienceDirect

Bioorganic & Medicinal Chemistry

journal homepage: www.elsevier.com/locate/bmc

# Inhibition of *Mycobacterium tuberculosis* InhA: Design, synthesis and evaluation of new di-triclosan derivatives

Tom Armstrong[a], Malcolm Lamont[a], Alice Lanne[b], Luke J. Alderwick[b], Neil R. Thomas[a,*]

[a] Biodiscovery Institute, School of Chemistry, University of Nottingham, University Park, Nottingham NG7 2RD, United Kingdom
[b] Institute of Microbiology and Infection, School of Bioscience, University of Birmingham, Birmingham B15 2TT, United Kingdom

ARTICLE INFO

*Keywords:*
InhA
Triclosan
Triazole
Isoniazid
*Mycobacterium tuberculosis*
TB

ABSTRACT

Multi-drug resistant tuberculosis (MDR-TB) represents a growing problem for global healthcare systems. In addition to 1.3 million deaths in 2018, the World Health Organisation reported 484,000 new cases of MDR-TB. Isoniazid is a key anti-TB drug that inhibits InhA, a crucial enzyme in the cell wall biosynthesis pathway and identical in *Mycobacterium tuberculosis* and *M. bovis*. Isoniazid is a pro-drug which requires activation by the enzyme KatG, mutations in KatG prevent activation and confer INH-resistance. 'Direct inhibitors' of InhA are attractive as they would circumvent the main clinically observed resistance mechanisms. A library of new 1,5-triazoles, designed to mimic the structures of both triclosan molecules uniquely bound to InhA have been synthesised. The inhibitory activity of these compounds was evaluated using isolated enzyme assays with **2** (5-chloro-2-(4-(5-(((4-(4-chloro-2-hydroxyphenoxy)benzyl)oxy)methyl)-1H-1,2,3-triazol-1-yl)phenoxy)phenol) exhibiting an $IC_{50}$ of 5.6 μM. Whole-cell evaluation was also performed, with **11** (5-chloro-2-(4-(5-(((4-(cyclopropylmethoxy)benzyl)oxy)methyl)-1H-1,2,3-triazol-1-yl)phenoxy)phenol) showing the greatest potency, with an $MIC_{99}$ of 12.9 μM against *M. bovis*.

## 1. Introduction

Tuberculosis (TB) is one the leading global causes of mortality and is currently the world's deadliest infectious disease. In addition to the estimated 1.3 million deaths from TB in 2018, a further 0.25 million Human Immunodeficiency Virus-positive (HIV) individuals died as a result of co-infection with *Mycobacterium tuberculosis*.[1]

The current anti-TB treatment course relies on four drugs: isoniazid (INH), rifampicin (RIF), ethambutol (ETH) and pyrazinamide (PZA). The increasing prevalence of multi-drug resistant TB (MDR-TB) threatens to undermine the efficacy of this treatment regimen. MDR-TB infections are characterised as those displaying resistance to INH and RIF. In 2018, the WHO reported over 484,000 new MDR-TB infections. Additionally, 13,000 were classified as extensively drug resistant (XDR-TB) meaning they were also insensitive to any fluoroquinolone and at least one of the second-line injectable drugs.[2–4] This emerging resistance is further exacerbated by the lack of novel drugs coming through the pipeline, with only three new drugs entering the clinic in the last 40 years (delamanid, pretomanid and bedaquiline).[5,6]

Mycobacteria's dense and complex cell wall represents one of the main reasons for the hardiness of the bacteria. The relative impermeability of the Mycobacterial cell wall can primarily be attributed to its mycolic acid component. This waxy layer consists of long chain ($\sim C_{50\text{-}90}$) α-branched, β-hydroxylated fatty acids. This barrier not only hinders the passage of small molecules into the cell, but also provides protection from the host's immune response.[7]

The frontline drug INH elicits its biological effects through disruption of the mycolic acid biosynthetic pathway, *via* inhibition of the enzyme InhA.[8] InhA is a nicotinamide adenine dinucleotide (NADH)-dependent enoyl acyl carrier reductase which catalyses the chemoselective reduction of its 2-*trans*-enoyl-ACP substrate. The enzyme has an identical amino acid sequence (and hence structure) in *M. tuberculosis* and *M. bovis*, the main causative agents of tuberculosis in humans and dairy cattle respectively. INH is actually a pro-drug which requires activation before it can inhibit mycolic acid biosynthesis (Fig. 1).

Initially, the catalase peroxidase enzyme, KatG converts INH to its

*Abbreviations:* ETH, ethambutol; GOLD, Genetic Optimisation for Ligand Docking; HIV, human immunodeficiency virus; HPLC, high-performance liquid chromatography; INH, isoniazid; MDR-TB, multi-drug resistant tuberculosis; NAD, nicotinamide adenine dinucleotide (oxidised form); NADH, nicotinamide adenine dinucleotide (reduced form); PZA, pyrazinamide; RIF, rifampicin; RuAAC, ruthenium-catalysed azide alkyne cycloaddition, TB, tuberculosis; TCS, triclosan; XDR-TB, extensively drug-resistant tuberculosis

* Corresponding author.
*E-mail address:* neil.thomas@nottingham.ac.uk (N.R. Thomas).

https://doi.org/10.1016/j.bmc.2020.115744
Received 10 July 2020; Received in revised form 24 August 2020; Accepted 27 August 2020
Available online 08 September 2020

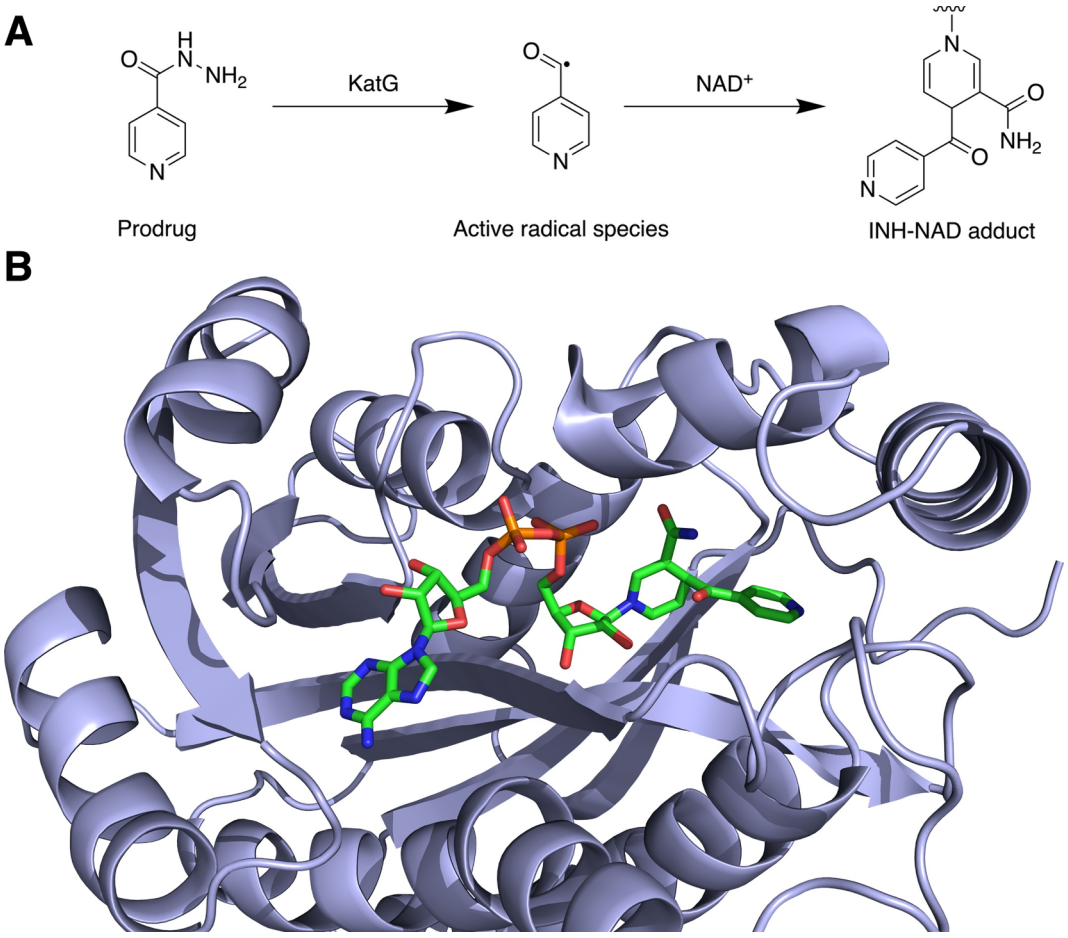


**Fig. 1.** (A) The structure of key anti-TB drug INH and the pathway through which it elicits its biological effects. (B) Crystal structure of the INH-NAD adduct bound to InhA showing how the adduct blocks the substrate binding cavity (PDB: 1ZID).

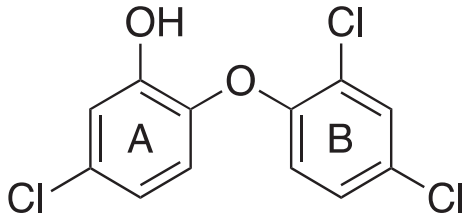


**Fig. 2.** The structure of TCS and the denotation of the A and B rings.

corresponding isonicotinyl radical species. Upon activation, INH forms a covalent adduct with the InhA co-factor which in turn blocks the active site, preventing substrate binding.[9,10] A single KatG point mutation, S315T, is sufficient to render INH inactive and has been implicated in up to 95% of INH resistant clinical isolates examined.[11,12] With this in mind, the development of 'direct InhA inhibitors' represents a compelling approach for the discovery of new anti-TB drugs.[13–16] Direct inhibitors refer to compounds which, unlike INH, do not require prior activation to exert their inhibitory effects. These inhibitors would circumvent the current resistance mechanisms and could be used to treat resistant infections. One such direct inhibitor is the small molecule, broad spectrum antibiotic triclosan (TCS, Fig. 2). TCS is a moderate, reversible inhibitor of InhA and has formed the basis of a number of studies, using its scaffold in the development of more potent inhibitors.[17,18]

Crystallographic studies have highlighted an unusual binding trait for the TCS:InhA complex. Two molecules of TCS are able to occupy the InhA active site (PDB: 1P45, Fig. 3), something not replicated in homologous proteins from other bacteria.[19] Inspection of the crystal structure reveals that the **TCS2** molecule lies only ~4.2 Å away from the **TCS1** moiety (Fig. 3). This suggests that through modification of the B-ring, it may be possible to obtain TCS derivatives which are capable of occupying both binding sites through a single molecule, potentially producing a more potent and selective inhibitor for InhA, that also benefits from a lower entropic cost to binding.

In this article, we report the *in silico* design, synthesis and characterization of a series of novel TCS derivatives bearing a 1,5-triazole group attached to the B-ring. These compounds were designed to occupy both of the TCS binding sites observed in the 1P45 crystal structure. Biological evaluation was performed using an isolated InhA enzyme assay and whole-cell screening against *M. bovis*.

The first step in designing TCS analogues which could anchor into both binding sites was identifying a suitable linker to connect the two fragments. It was vital that the linker did not disrupt the experimentally observed binding mode for **TCS1**, while at the same time the linker geometry had to direct the attached fragment back into the **TCS2** binding region. To this end, it was thought that a disubstituted 1,2,3-triazole ring would be an appropriate motif. It was hoped that the rigid nature of the triazole scaffold would direct any substituent group back into the **TCS2** binding site. This notion was explored using the **G**enetic **O**ptimisation for **L**igand **D**ocking (GOLD) platform.[20] Two test compounds, a 1,4 and a 1,5-triazole, were designed and both were docked into the InhA active site (PDB: 1P45). The binding poses obtained are shown below in Fig. 4.

As demonstrated in Fig. 4, when the two fragments are connected through a 1,5-triazole unit (**2**), the TCS-like binding mode is retained, and the secondary fragment occupies the same space as the **TCS2**

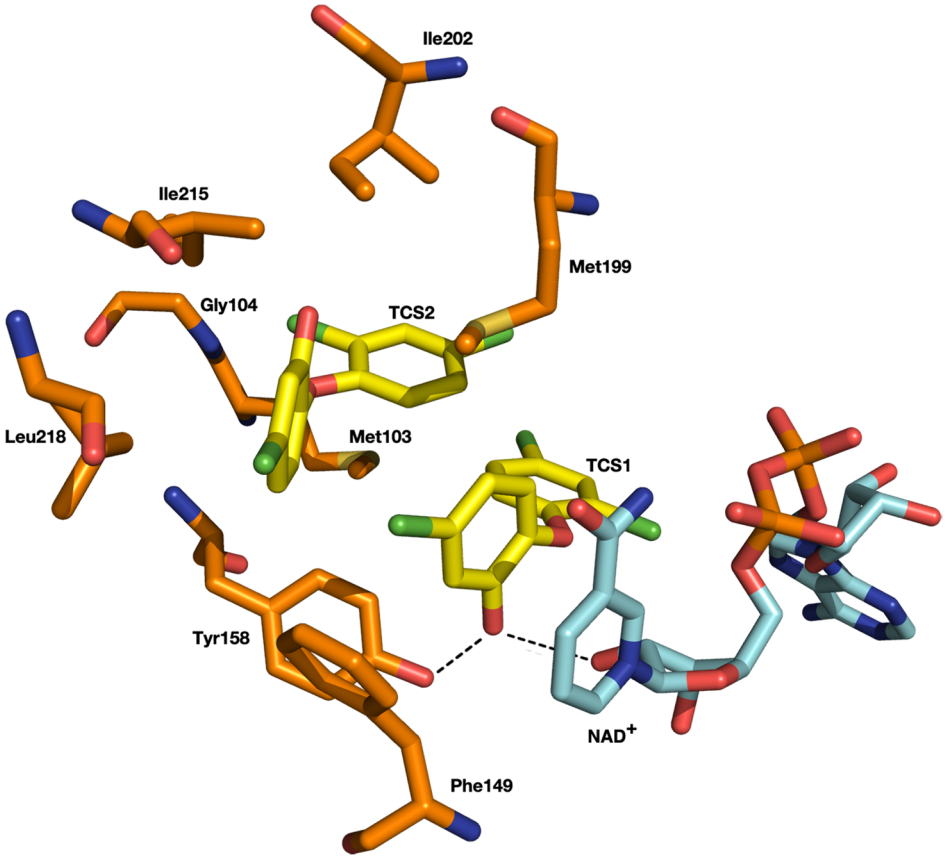


**Fig. 3.** X-ray structure showing two TCS molecules bound to the InhA active site. Residues are shown with orange carbons, $NAD^+$ is shown with teal carbons, TCS are shown with yellow carbons. H-bonds are shown by dashed-black lines. (PDB: 1P45).

moiety. The 1,4-triazole (**1**) did not generate a suitable structure and the B-ring modification resulted in a perturbation of the TCS binding mode, including loss of the key hydrogen bonding network shown in Fig. 3. This is of particular importance as this H-bonding network is conserved amongst all potent direct InhA inhibitors, with the exception of the methyl-thiazole compound class.[19,21–23]

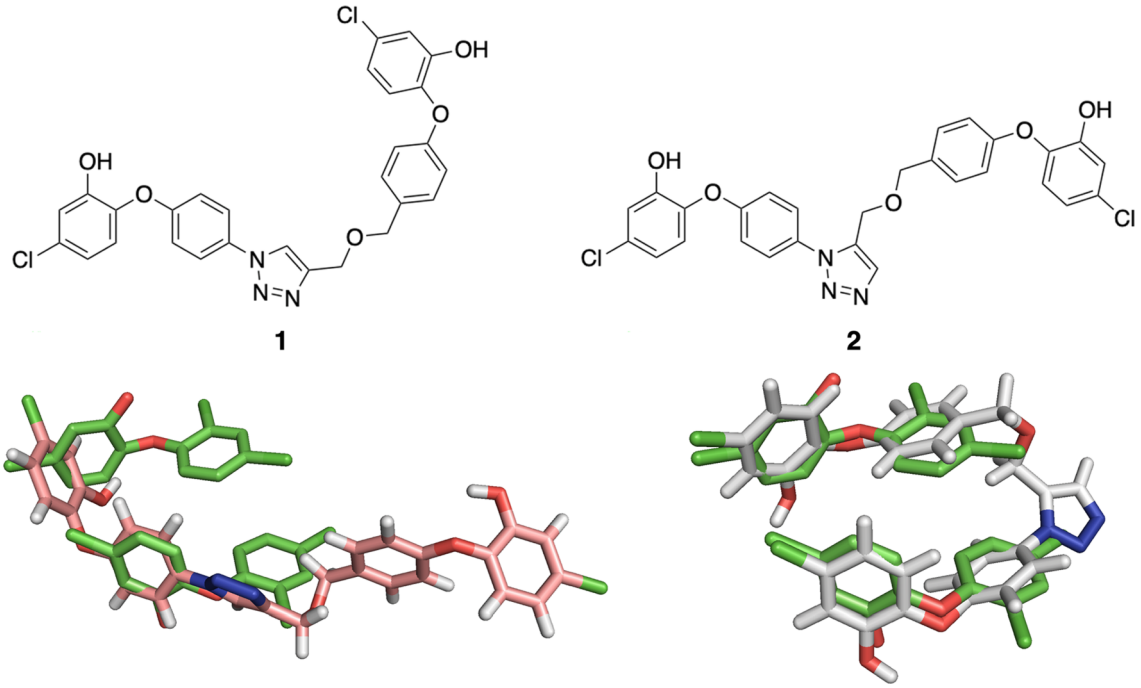


**Fig. 4.** The structures of two basic TCS-triazole compounds and their docking poses generated by GOLD, this shows the overlap between the designed compounds and the two TCS moieties found in the active site. (PDB: 1P45).

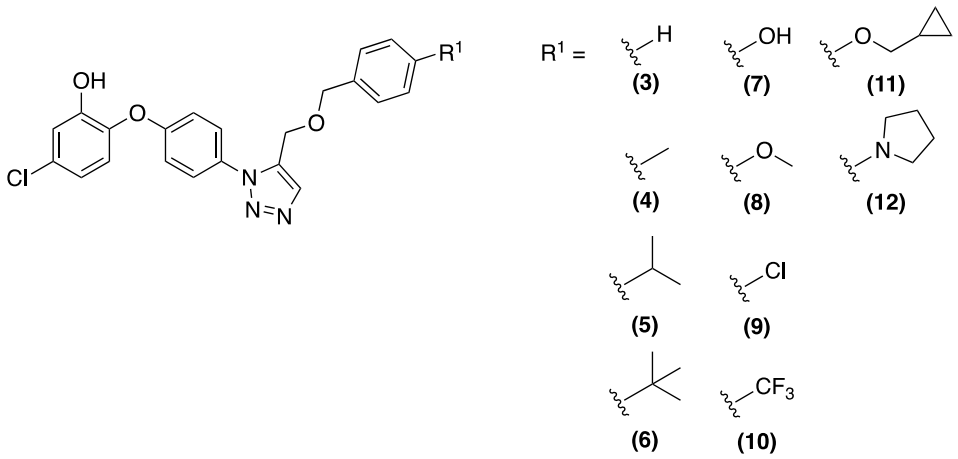


**Fig. 5.** Design strategy for novel TCS-based InhA inhibitors.

With this information in hand, a range of compounds bearing a single aromatic ring attached through the 1,5-triazole motif were also designed (Fig. 5). Previous studies have demonstrated that the B-ring Cl atoms are not required for potent InhA inhibition and so they were removed in an attempt to control the lipophilicity of the target compounds.[18,24]

The synthesis of biaryl azide **16** is shown in Scheme 1. The initial biaryl scaffold was assembled through an $S_NAr$ reaction using 1-fluoro-4-nitrobenzene and 4-chloro-2-methoxyphenol, furnishing **13** in near quantitative yields. Sequential $BBr_3$ mediated ether demethylation and nitro reduction with $Zn/NH_4Cl$ gave amine **15** in a good yield over two steps. Finally, functional group interconversion under the mild conditions first reported by Barral *et al.* provided the target azide **16** in a good yield.[25]

The synthesis of alkyne-bearing TCS fragment **22** is shown in Scheme 2. The biphenyl scaffold **17** was assembled in a similar fashion to the corresponding nitro compound **13**, in a good yield. Cleavage of the methyl ether was performed using AcOH and HBr at elevated temperatures, generating **18** in a modest yield. This method was used due to the instability of the benzaldehyde group that was observed when demethylation was attempted with $BBr_3$. The newly exposed phenol was then reprotected using MOMCl in a good yield. Benzaldehyde **19** was reduced to its corresponding benzyl alcohol using $NaBH_4$ before etherification using NaH and propargyl bromide, giving ether **21** in good yield over two steps. The phenol functionality was then unmasked using 6 M HCl to furnish the alkyne-bearing TCS fragment **22** in a near quantitative yield.

The selective formation of 1,5-triazoles can be achieved through the use of a ruthenium catalysed azide-alkyne cycloaddition (RuAAC), this methodology has seen an increasing numbers of examples in the literature over the last decade.[26,27] With **22** and **16** in hand, the 1,5-triazole motif was assembled *via* a RuACC, using $Cp^*RuCl(PPh_3)_2$ in 1,4-dioxane (Scheme 3).

The RuAAC reaction furnished **2** in an acceptable yield, following reverse phase high performance liquid chromatography (HPLC) purification. The identity of the product was confirmed as a 1,5-triazole using the NMR methods previously discussed by Creary *et al.*[28] Following the synthesis of **2**, the aforementioned truncated analogues were synthesised from the azide **16** and alkyne fragments (**23–32**, synthesis detailed in supplementary information), using the same RuAAC conditions, giving the desired 1,5-triazoles in moderate yields after HPLC (Scheme 4).

An isolated enzyme assay was used to assess the inhibitory properties of the compounds synthesised. Initial screening was performed at 50 μM with 150 nM of InhA from *M. tuberculosis* using a standard UV absorbance assay that has been widely used in the identification of

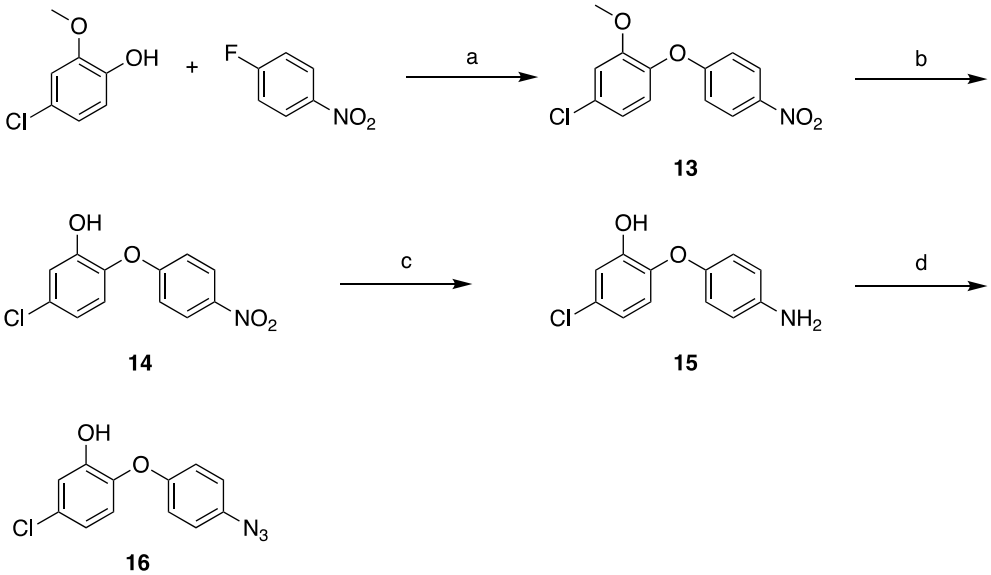


**Scheme 1.** Reagents and conditions: (a) $K_2CO_3$, DMF, 130 °C, 18 h, 95%; (b) $BBr_3$, $CH_2Cl_2$, 0 °C - > r.t., $N_2$, 3 h, 89%; (c) Zn, $NH_4Cl$, MeOH, r.t., 18 h, 75%; (d) $^tBuONO$, $TMSN_3$, ACN, 0 °C - > r.t., 3 h, 80%.

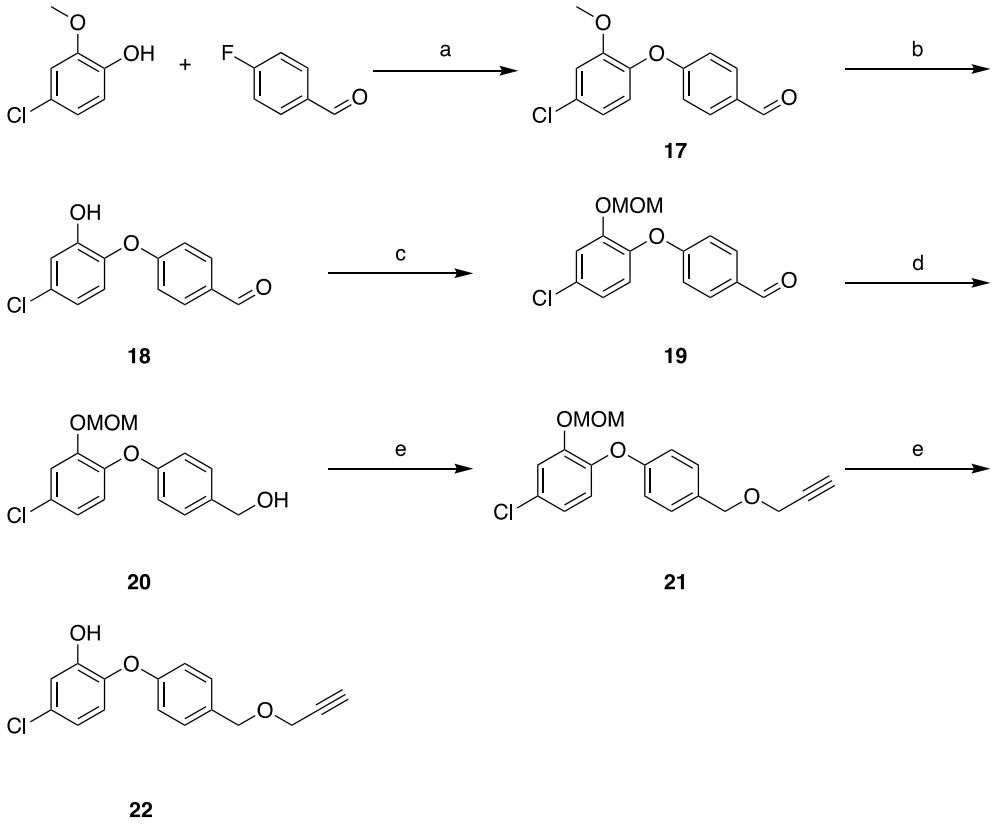


**Scheme 2.** Reagents and conditions: (a) $K_2CO_3$, DMF, 130 °C, 18 h, 92%; (b) AcOH, HBr, 140 °C, 18 h, 38%; (c) MOMCl, DIPEA, $CH_2Cl_2$, r.t., 18 h, 86%; (d) $NaBH_4$, MeOH, 0 °C - > r.t., 4 h, quant.; (e) NaH, propargyl bromide, DMF, 0 °C - > r.t., 18 h, 79%; (f) 6 M HCl (aq), MeOH, 70 °C, 2 h, 90%.

novel InhA inhibitors. Assays were performed using 2-*trans*-octenoyl CoA as a mimic for the enzyme's natural substrate.[29] All compounds evaluated were of above 90% purity as determined by analytical HPLC.

The inhibitory activity observed for compounds **2–12** is summarised in Table 1, these results indicate a number of the compounds tested showed moderate inhibition of InhA at 50 μM. Moving from H- > Me- > $^{i}$Pr (**3**- > **5**) results in increased inhibition, however, the introduction of a $^{t}$Bu (**6**) leads to a significant reduction in enzyme inhibition, suggesting that such a bulky group results in major clashes with the protein. This loosely correlates with the fitness scores, with compound **6** showing a lower fitness score than **5**. The possibility that this region is size sensitive is further supported by the fact that compounds **8**, **10** and **12**, all of which bear relatively small R groups, show moderate inhibition. The most potent compound was **2** which showed a total reduction in enzyme activity at 50 μM.

The predicted binding mode for **2** is shown in Fig. 6. This binding pose shows how the 'front' TCS fragment is able to engage the $NAD^+$ co-factor and Tyr158 through the key hydrogen bonding network. The 1,5-triazole architecture directs the second TCS fragment back towards the substrate binding loop, where a number of hydrophobic contacts are made. Further evaluation of **2** showed it exhibits an $IC_{50}$ of 5.6 ± 0.8 μM (n = 3). This represents a modest improvement on TCS ($IC_{50}$ = 9.2 ± 1.3 μM, n = 3) recorded in experiments conducted in parallel and widely reported in the literature.[30]

Whole-cell evaluation of all 12 compounds was undertaken to investigate the correlation between isolated enzyme activity and whole-cell potency. Compounds were initially assessed for growth inhibition against *Mycobacterium bovis* at a fixed concentration of 40 μM. Results are shown in Table 2.

Disappointingly, the isolated assay potency of **2** towards InhA did not correlate to whole-cell potency. This could possibly be attributed to inability to pass through the dense mycobacterial cell wall, or other factors such as efficient transport by efflux pumps.[31,32] It is possible that reintroducing the *ortho* Cl atom to the B-ring (giving a compound with a cLogP 6.61) could result in greater whole-cell potency, although the previous QSAR study by Sivaraman *et al.*[24] indicate that this chlorine is not critical, this is something that will be explored going forward. Of the 12 compounds tested, **11** showed the greatest potency, with 99% growth inhibition at 40 μM. This compound was subject to further evaluation to determine its $MIC_{99}$ (Fig. 7).

Compound **11** displayed an $MIC_{99}$ of 12.9 ± 5.0 μM (6.2 μg $mL^{-1}$, n. = 3). Clearly there is a disconnect between the activity of **11** in

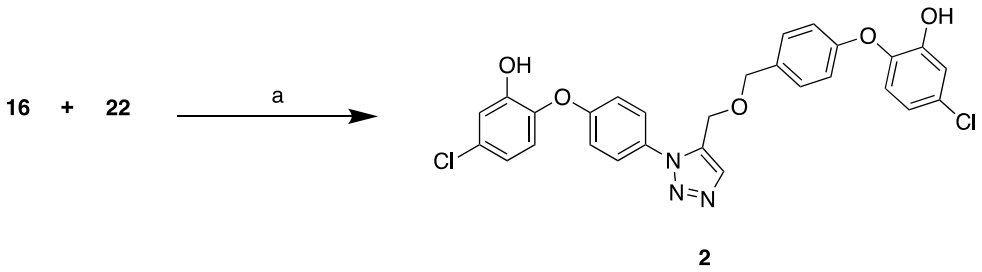


**Scheme 3.** Reagents and conditions: (a) Cp*RuCl($PPh_3$)$_2$, 1,4-dioxane, 60 °C, $N_2$, 18 h, 17%.

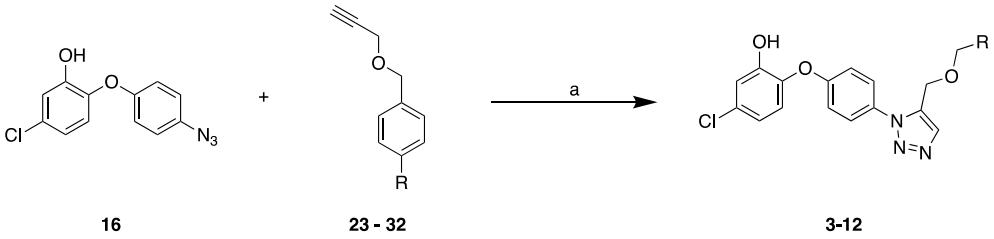


16 23 - 32 3-12

**Scheme 4.** Reagents and conditions: (a) Cp*RuCl($PPh_3$)$_2$, 1,4-dioxane, 60 °C, $N_2$, 18 h, 5–33%.

**Table 1**
Inhibitory data for compounds tested using an isolated enzyme assay, conducted at 50 μM. GOLD fitness scores are also included for each compound. Inhibition values are an average of duplicate assays.

| Compound | GOLD Fitness Score | Inhibition/% |
|---|---|---|
| **2** | 87.7 | 100 |
| **3** | 65.2 | 12 |
| **4** | 73.5 | 38 |
| **5** | 77.8 | 72 |
| **6** | 74.0 | 6 |
| **7** | 69.0 | 13 |
| **8** | 76.7 | 44 |
| **9** | 73.2 | 0 |
| **10** | 75.6 | 47 |
| **11** | 80.7 | 11 |
| **12** | 83.6 | 42 |
| **TCS** | 70.8 | 92 |

**Table 2**
Inhibition data for all compounds tested against Mycobacterium bovis at 40 μM, results are shown as an average of 3 assays.

| Compound | Inhibition/% | cLogP |
|---|---|---|
| **2** | 20 | 5.80 |
| **3** | 3 | 5.11 |
| **4** | −6 | 5.43 |
| **5** | 15 | 5.89 |
| **6** | 20 | 6.11 |
| **7** | 0 | 4.37 |
| **8** | 40 | 5.03 |
| **9** | 4 | 5.61 |
| **10** | 19 | 6.09 |
| **11** | 99 | 6.07 |
| **12** | 23 | 5.95 |
| **TCS** | 70 | 4.98[38] |

isolated enzyme assays and its performance in the whole-cell screening tests. This suggests that **11** has other off-target sites within the bacteria which result in significant potency. At high concentrations TCS has been reported to act as a mitochondrial uncoupling, cell membrane permeator and to cause disruption to both lipid and protein biosynthesis.[18] Further work will be required to elucidate the main biological target(s) of **11**.

As previously mentioned, TCS has formed the basis for a number of SAR studies towards potent inhibitors of InhA. The most common

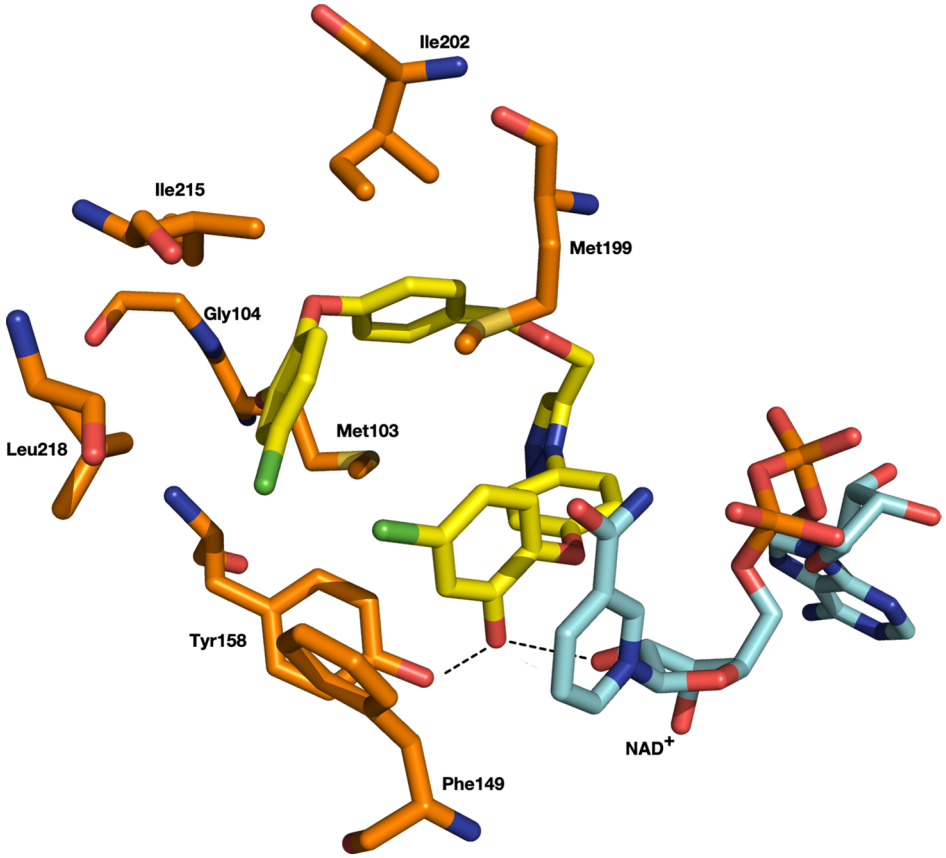


**Fig. 6.** Predicted binding mode for **2**. Residues are shown with orange carbons, $NAD^+$ is shown with teal carbons, **2** is shown with yellow carbons. H-bonds are shown by dashed-black lines. (PDB: 1P45).

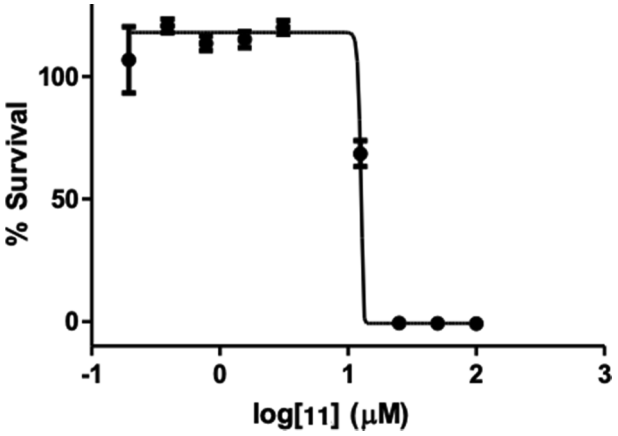


**Fig. 7.** $MIC_{99}$ curve for **11**.

modification is replacement of the A-ring Cl atom with various hydrophobic groups. Comprehensive B-ring modifications remain relatively unexplored.[33–35] Two examples of previously disclosed direct InhA inhibitors are shown in Fig 8.[35,36] Compound **2** is similar in concept to **33**, recently reported by Rodriguez *et al.*, which sought to merge two TCS molecules in a macrocyclic arrangement. Compounds **33** and **2** have similar $IC_{50}$ values, which would be expected as they both target the same binding sites.

In terms of $MIC_{99}$ data, in this study, **11** showed significant potency in whole-cell assays with an $MIC_{99}$ value of 12.9 μM, this value is approaching the $MIC_{99}$ of **34** (6.6 μM). It is possible that, following the elucidation of **11**'s target, its potency could be further improved to the match or exceed the activity of **34**.

The rational *in silico* design, synthesis and characterization of a novel series of triazole-bearing TCS derivatives is reported. These compounds were designed to exploit the large volume of the InhA active site and occupy both TCS binding sites observed in the PDB: 1P45 crystal structure. Docking results suggested that these compounds would be able to occupy both of the TCS binding regions, possibly giving a direct inhibitor of Mycobacterial InhA with higher affinity and selectivity than TCS. Enzyme assays on purified *M. tuberculosis* InhA were used to evaluate the compounds synthesised, with the most potent showing an $IC_{50}$ of 5.6 ± 0.8 μM which is similar to that of TCS. Whole-cell evaluation against *M. bovis* showed the most potent compound was **11** which displayed an MIC of 12.9 ± 5.0 μM, despite only showing 11% inhibition at 50 μM in isolated enzyme assays.

## Author Contributions

T.A. synthesised all compounds, performed enzyme assays, analysed data and wrote the manuscript. M.L. expressed & purified InhA and performed enzyme assays. A.L. performed whole-cell screening assays and analysed data. L.J.A. supervised the whole-cell screening assays. N.R.T. came up with the initial drug design concept, supervised the synthetic research, contributed to writing and editing the manuscript.

## Funding

T.A. is supported by the Wellcome Trust Antimicrobials and Antimicrobial Resistance (AAMR) doctoral training programme Birmingham/Nottingham [203974/Z/17/A].

M.L. is supported by a Biotechnology and Biological Sciences Research Council doctoral training studentship [Grant Number BB/M008770/1].

A.L. is supported by the Wellcome Trust Antimicrobials and Antimicrobial Resistance (AAMR) doctoral training programme Birmingham/Nottingham [215154/Z/18/Z].

## Declaration of Competing Interest

The authors declare that they have no known competing financial interests or personal relationships that could have appeared to influence the work reported in this paper.

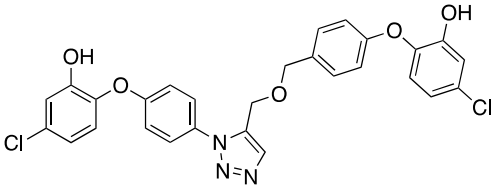

**2**
M.W: 550.39 g $mol^{-1}$
$Mtb_{InhA}$ $IC_{50}$ (μM): 5.6 ± 0.8
$MIC_{99}$ (μM): >80

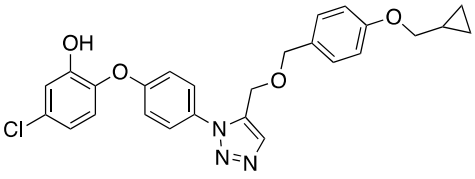

**11**
M.W: 477.95 g $mol^{-1}$
$Mtb_{InhA}$ $IC_{50}$ (μM): >50
$MIC_{99}$ (μM): 12.9 ± 5.0

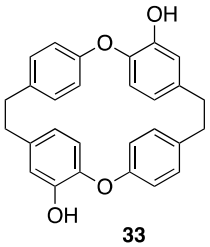

**33**
M.W: 424.50 g $mol^{-1}$
$Mtb_{InhA}$ $IC_{50}$ (μM): 4.7 ± 0.4
$MIC_{99}$ (μM): 94.2*

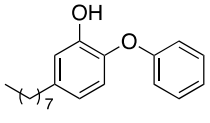

**34**
M.W: 289.43 g $mol^{-1}$
$Mtb_{InhA}$ $IC_{50}$ (μM): 0.005 ± 0.0003
$MIC_{99}$ (μM): 6.6 ± 1.7

*Standard deviation not reported by authors

**Fig. 8.** The structures of previously disclosed TCS-based inhibitors of InhA and their biological activities.

## Acknowledgements

The InhA:pET15a construct was kindly provided by Prof. Peter Tonge (SUNY, Stonybrook, NY, USA).[37]

## Appendix A. Supplementary material

Experimental details are reported including: full synthetic procedures and characterization data for all compounds. NMR spectra and analytical HPLC traces of key compounds **2** and **11** are included. Methods for protein expression, purification, isolated enzyme activity assay conditions, $IC_{50}$ curve for compound **2** and whole-cell screening methods are also included.

Supplementary data to this article can be found online at https://doi.org/10.1016/j.bmc.2020.115744.

## References

1. World Health Organisation. Global Tuberculosis Report; 2019.
2. Bastos ML, Lan Z, Menzies D. An updated systematic review and meta-analysis for treatment of multidrug-resistant tuberculosis. *Eur Respir J.* 2017;49:1600803.
3. Günther G. Multidrug-resistant and extensively drug-resistant tuberculosis: a review of current concepts and future challenges. *Clin Med (Lond).* 2014;14:279–285.
4. Pontali E, D'Ambrosio L, Centis R, Sotgiu G, Migliori GB. Multidrug-resistant tuberculosis and beyond: an updated analysis of the current evidence on bedaquiline. *Eur Respir J.* 2017;49:1700146.
5. Deoghare S. Bedaquiline: a new drug approved for treatment of multidrug-resistant tuberculosis. *Indian J. Pharmacol.* 2013;45:536–537.
6. Xavier A, Lakshmanan M. Delamanid: A new armor in combating drug-resistant tuberculosis. *J Pharmacol Pharmacother.* 2014;5:222–224.
7. Zhai W, Wu F, Zhang Y, Fu Y, Liu Z. The immune escape mechanisms of mycobacterium tuberculosis. *Int J Mol Sci.* 2019;20:340.
8. Marrakchi H, Laneelle G, Quemard AK. InhA, a target of the antituberculous drug isoniazid, is involved in a mycobacterial fatty acid elongation system, FAS-II. *Microbiology.* 2000;146:289–296.
9. Rozwarski DA, Grant GA, Barton DH, Jacobs Jr WR, Sacchettini JC. Modification of the NADH of the isoniazid target (InhA) from Mycobacterium tuberculosis. *Science.* 1998;279:98–102.
10. Timmins GS, Deretic V. Mechanisms of action of isoniazid. *Mol Microbiol.* 2006;62:1220–1227.
11. Zhang Y, Heym B, Allen B, Young D, Cole S. The catalase—peroxidase gene and isoniazid resistance of Mycobacterium tuberculosis. *Nature.* 1992;358:591–593.
12. Zhao X, Yu H, Yu S, Wang F, Sacchettini JC, Magliozzo RS. Hydrogen peroxide-mediated isoniazid activation catalyzed by mycobacterium tuberculosis catalase−-peroxidase (KatG) and Its S315T Mutant. *Biochemistry.* 2006;45:4131–4140.
13. Manjunatha UH, Rao SP, Kondreddi RR, et al. Direct inhibitors of InhA are active against Mycobacterium tuberculosis. *Sci Transl Med.* 2015;7:269ra3.
14. Martínez-Hoyos M, Perez-Herran E, Gulten G, et al. Antitubercular drugs for an old target: GSK693 as a promising InhA direct inhibitor. *EBioMedicine.* 2016;8:291–301.
15. Rozman K, Sosic I, Fernandez R, et al. A new 'golden age' for the antitubercular target InhA. *Drug Discov Today.* 2017;22:492–502.
16. Chetty S, Ramesh M, Singh-Pillay A, Soliman ME. Recent advancements in the development of anti-tuberculosis drugs. *Bioorg Med Chem Lett.* 2017;27:370–386.
17. Parikh SL, Xiao G, Tonge PJ. Inhibition of InhA, the Enoyl Reductase from Mycobacterium tuberculosis, by Triclosan and Isoniazid. *Biochemistry.* 2000;39:7645–7650.
18. Vosatka R, Kratky M, Vinsova J. Triclosan and its derivatives as antimycobacterial active agents. *Eur J Pharm Sci.* 2018;114:318–331.
19. Kuo MR, Morbidoni HR, Alland D, et al. Targeting tuberculosis and malaria through inhibition of Enoyl reductase: compound activity and structural data. *J Biol Chem.* 2003;278:20851–20859.
20. Jones G, Willett P, Glen RC, Leach AR, Taylor R. Development and validation of a genetic algorithm for flexible docking. *J Mol Biol.* 1997;267:727–748.
21. Shirude PS, Madhavapeddi P, Naik M, et al. Methyl-thiazoles: a novel mode of inhibition with the potential to develop novel inhibitors targeting InhA in Mycobacterium tuberculosis. *J Med Chem.* 2013;56:8533–8542.
22. Ng PS, Manjunatha UH, Rao SPS, et al. Structure activity relationships of 4-hydroxy-2-pyridones: A novel class of antituberculosis agents. *Eur J Med Chem.* 2015;106:144–156.
23. Encinas L, O'Keefe H, Neu M, et al. Encoded library technology as a source of hits for the discovery and lead optimization of a potent and selective class of bactericidal direct inhibitors of mycobacterium tuberculosis InhA. *J Med Chem.* 2014;57:1276–1288.
24. Sivaraman S, Sullivan TJ, Johnson F, et al. Inhibition of the bacterial enoyl reductase FabI by triclosan: a structure-reactivity analysis of FabI inhibition by triclosan analogues. *J Med Chem.* 2004;47:509–518.
25. Barral K, Moorhouse AD, Moses JE. Efficient conversion of aromatic amines into azides: a one-pot synthesis of triazole linkages. *Org Lett.* 2007;9:1809–1811.
26. Boren BC, Narayan S, Rasmussen LK, et al. Ruthenium-catalyzed azide−alkyne cycloaddition: scope and mechanism. *J Am Chem Soc.* 2008;130:8923–8930.
27. Johansson JR, Beke-Somfai T, Said Stålsmeden A, Kann N. Ruthenium-catalyzed azide alkyne cycloaddition reaction: scope, mechanism, and applications. *Chem Rev.* 2016;116:14726–14768.
28. Creary X, Anderson A, Brophy C, Crowell F, Funk Z. Method for assigning structure of 1,2,3-triazoles. *J Org Chem.* 2012;77:8756–8761.
29. He X, Alian A, Stroud R, Ortiz de Montellano PR. Pyrrolidine carboxamides as a novel class of inhibitors of enoyl acyl carrier protein reductase from Mycobacterium tuberculosis. *J Med Chem.* 2006;49:6308–6323.
30. Slepikas L, Chiriano G, Perozzo R, et al. In silico driven design and synthesis of rhodanine derivatives as novel antibacterials targeting the enoyl reductase InhA. *J Med Chem.* 2016;59:10917–10928.
31. Szumowski JD, Adams KN, Edelstein PH, Ramakrishnan L. Antimicrobial efflux pumps and Mycobacterium tuberculosis drug tolerance: evolutionary considerations. *Curr Top Microbiol Immunol.* 2013;374:81–108.
32. Balganesh M, Dinesh N, Sharma S, Kuruppath S, Nair AV, Sharma U. Efflux pumps of mycobacterium tuberculosis play a significant role in antituberculosis activity of potential drug candidates. *Antimicrob Agents Chemother.* 2012;56:2643–2651.
33. He X, Alian A, Ortiz de Montellano PR. Inhibition of the Mycobacterium tuberculosis enoyl acyl carrier protein reductase InhA by arylamides. *Bioorg Med Chem.* 2007;15:6649–6658.
34. Stec J, Vilchèze C, Lun S, et al. Biological evaluation of potent triclosan-derived inhibitors of the enoyl-acyl carrier protein reductase InhA in drug-sensitive and drug-resistant strains of mycobacterium tuberculosis. *ChemMedChem.* 2014;9:2528–2537.
35. Sullivan TJ, Truglio JJ, Boyne ME, et al. High affinity InhA inhibitors with activity against drug-resistant strains of Mycobacterium tuberculosis. *ACS Chem Biol.* 2006;1:43–53.
36. Rodriguez F, Saffon N, Sammartino JC, Degiacomi G, Pasca MR, Lherbet C. First triclosan-based macrocyclic inhibitors of InhA enzyme. *Bioorg Chem.* 2020;95:103498.
37. Parikh S, Moynihan DP, Xiao G, Tonge PJ. Roles of tyrosine 158 and lysine 165 in the catalytic mechanism of InhA, the enoyl-ACP reductase from Mycobacterium tuberculosis. *Biochemistry.* 1999;38:13623–13634.
38. Han J, Cao Z, Gao W. Remarkable sorption properties of polyamide 12 microspheres for a broad-spectrum antibacterial (triclosan) in water. *J Mater Chem A.* 2013;1(16):4941–4944.